THE DI-B IN-SITU DIFFUSION EXPERIMENT AT MONT TERRI: RESULTS AND MODELING

J. M. Soler[1], J. Samper[2], A. Yllera[3], A. Hernández[3], A. Quejido[3], M. Fernández[3], C. Yang[2], A. Naves[2], P. Hernán[4], P. Wersin[5]

1. Institut de Ciències de la Terra "Jaume Almera" (CSIC), Lluís Solé i Sabarís s/n, 08028 Barcelona, Spain. Fax: +34-934110012. E-mail: jsoler@ija.csic.es. Corresponding author.
2. Universidade da Coruña, Campus de Elviña, 15192 A Coruña, Spain (jsamper@udc.es)
3. CIEMAT, Avda. Complutense 22, 28040 Madrid, Spain (abel.yllera@ciemat.es)
4. ENRESA, Emilio Vargas 7, 28043 Madrid, Spain (pher@enresa.es)
5. NAGRA, Hardstrasse 73, CH-5430 Wettingen, Switzerland (paul.wersin@nagra.ch)

Abstract

The main objective of the DI-B experiment was to study the transport and retention properties of selected tracers in the Opalinus Clay at the Mont Terri underground rock laboratory, but using only non radioactive species. The selected tracers were HDO (water), I^- (anionic species), $^6Li^+$ (non- or weakly-sorbing cation) and $^{87}Rb^+$ (strongly-sorbing cation). The diffusion experiment was carried out in the DI niche (shaly facies). The experiment was performed as a single point dilution test by injecting stable tracers into a packed-off section at the bottom of a vertical borehole 7.7 m deep. The dip of the bedding was 32º to the SE. The length of the borehole interval where tracers were injected was 0.6 m and the radius of the borehole was 0.038 m. A volume of rock around the injection interval was overcored after the end of the experiment, allowing the measurement of tracer distribution profiles. The experiment lasted slightly over one year. The results of the experiment included the evolution of tracer concentrations in the injection system and tracer distribution profiles in the rock. Two and three-dimensional modeling of the results has been performed using the CRUNCH and CORE^{3D} reactive transport codes, respectively. The experiment was designed so the length of the injection interval was larger than tracer transport distances. This experimental setup favors, in principle, a simple 2D interpretation of the results, since diffusion occurs mainly along bedding planes. The results for the conservative tracers from 2D modeling (CRUNCH) are $De_{\|}=5.0x10^{-11}$ m^2/s, $\phi=0.16$ (HDO) and $De_{\|}=1.2x10^{-11}$ m^2/s, $\phi=0.09$ (I^-). The results from 3D modeling (CORE^{3D}) are $De_{\|}=4.0x10^{-11}$ m^2/s, $De_{\|}/De_{\perp}=4$, $\phi=0.15$ (HDO) and $De_{\|}=8.3x10^{-12}$ m^2/s, $De_{\|}/De_{\perp}=4$, $\phi=0.08$ (I^-). The difference in the results may be due to the different geometries (3D vs. 2D), to other aspects of the calculations or to how model and experiments are compared. A previous sensitivity analysis performed with the 3D model had shown that the effect of considering only diffusion along the bedding planes ($De_{\|}/De_{\perp}=100$) was relatively minor, causing only a significant effect on tracer distribution in the rock near the top and bottom edges of the injection interval. The differences between the two sets of results are small and confirm the smaller effective diffusion coefficient and accessible porosity of I^- with respect to HDO. The results corresponding to $^6Li^+$ and $^{87}Rb^+$ have also been modeled using both 2D and 3D approaches. For $^6Li^+$ ($C_0=3x10^{-5}$ mol/l), the best fit for both models was achieved with $De_{\|} \approx 7x10^{-11}$ m^2/s, Kd ≈ 0.2 l/kg and $\phi=0.15$-0.16. The De and Kd values are very similar to those obtained previously for Na^+ at Mont Terri. This Kd value is certainly larger than what was initially expected. Regarding $^{87}Rb^+$ ($C_0=3x10^{-7}$ mol/l), only three profiles were finally measured, and they showed significant variability. This variability has also been observed for

other strongly sorbing tracers (Cs^{+}, Co^{2+}) in the DI-A and DI-A2 in-situ experiments at Mont Terri. It has not been possible to obtain unique values for $De_{\|}$ and Kd for $^{87}Rb^{+}$, although strong sorption has been confirmed.

Introduction

Argillaceous formations are being considered as potential host rocks for the deep geological disposal of radioactive waste, mainly due to their low permeability and good sorption properties. Solute transport is dominated by diffusion in this type of rocks.

Within the framework of the Mont Terri Project, the study of the transport and retention properties of the Opalinus Clay Formation has been the focus of a major experimental effort. Chemical profiles of chloride, bromide, sodium, helium, deuterium and ^{18}O in the Opalinus Clay porewater at Mont Terri are consistent with slow diffusion from the saline Opalinus Clay porewater to the young groundwaters of the adjacent limestone formation (Degueldre et al., 2003; Rübel et al. 2002). The results obtained from a first in-situ diffusion experiment with conservative tracers (DI Experiment) showed that the transport properties for tritium (HTO) were consistent with through-diffusion measurements obtained on small-sized Opalinus Clay samples (Palut et al., 2003; Tevissen et al., 2004). The DI-A experiment made use of both conservative (HTO, I^-) and sorbing tracers ($^{22}Na^+$, Cs^+). The results (Wersin et al., 2004; Van Loon et al., 2004b; Wersin et al., 2006) showed a good agreement between laboratory and field results and confirmed the effect of anion exclusion on the transport properties of I^- (reduced effective diffusion coefficient and accessible porosity).

After the start of the DI-A experiment, the DI-B project was designed. The DI-B experiment was a Spanish Project led by Enresa and financed by Enresa and Nagra. One of its main objectives was to study the transport and retention properties of selected tracers in the Opalinus Clay, but using only non radioactive species. The selected tracers (Yllera et al., 2004) were HDO (water), I^- (anionic species), $^6Li^+$ (non- or weakly-sorbing cation) and $^{87}Rb^+$ (strongly-sorbing cation).

Experimental concept

The diffusion experiment was carried out in the BDI-B3 borehole located at the entrance of the DI niche in the Gallery 98 of the Mont Terri underground rock laboratory. This zone of the Mont Terri tunnel corresponds to the shaly facies of the Opalinus Clay, a few meters away from the underlying formation (Jurensis Marl, Toarcian). The in-situ diffusion experiment was performed as a single point dilution test by injecting stable tracers into a packed-off section at the bottom of a vertical borehole 7.7 m deep (Fig.1). The dip of the bedding was 32° to the SE. The length of the borehole interval where tracers were injected was 0.6 m and the radius of the borehole was 0.038 m. The experiment included downhole and

surface instrumentation. Downhole instrumentation consisted of a pneumatic single packer system with a porous screen made of sintered stainless steel mounted just below the packer at the bottom of the borehole. Surface instrumentation included a closed 316-l stainless steel circuit intended to circulate the synthetic porewater containing the tracers. To ensure that solution chemistry and pressure were in equilibrium with the rock, synthetic Opalinus Clay porewater (Table 1) without any added tracers was circulated during approximately 5 months prior to tracer injection. Injection and monitoring of tracers were done from the main tank through a valve system. The total volume of solution in the circulation system was about 30 liters. Further details regarding the experimental setup are reported by Yllera et al. (2004).

A volume of rock around the injection interval was overcored after the end of the experiment, allowing the measurement of tracer distribution profiles. The experiment lasted slightly over one year (417 days; Sept. 6th 2002 – Oct. 28th 2003). The removal of the overcore in the test interval was completed successfully with no core losses (Fig. 2(A)). Several sandy layers and a small tectonic fracture were observed in the overcore at the upper part of the interval. Such sandy layers, which are common in the shaly facies of the Opalinus clay, are probabably characterized by transport parameters different than those of the bulk claystone. Several subcores were taken from the overcore in order to obtain tracer concentration profiles along different directions from the pilot borehole. Fig. 2(A) shows a view image of the overcore of BDI-B3. Fig. 2(B) illustrates the location of the 12 profiles which were sampled from the overcore, while Fig. 2(C) shows also the bedding. Each subcore was sliced into a number of samples ranging from 9 to 12, each one having a thickness of 1 cm. Profiles 1–5 and 9 are horizontal and parallel to bedding; profiles 6, 7 and 8 are also horizontal but perpendicular to profiles 1–5 (32º angle with respect to bedding); profiles 10 and 11 are at an angle of 74º with respect to bedding; profile 12 is vertical, starting form the bottom of the borehole.

Every sliced sample of Opalinus Clay was weighed and placed into pre-weighed plastic (polyethylene) bottles containing 40 ml of deionized water. The bottles were closed and, previously to the chemical and isotopic analyses, shaken for two months in an orbital shaker at 4 ºC, until total disintegration of the solid. After that, the samples were centrifuged at 26300 g and the liquid fractions were separated from the solid phase for tracer analyses. The remaining solid fraction was kept for gravimetric determination of the moisture content by heating at 105 ºC until constant weight was achieved. The average moisture content for the samples was 6.77±0.71%.

The analyses of the aqueous extracts obtained from the solid (overcore) and liquid samples (monitoring from circulation tank) were performed as follows:

Deuterated water. The analyses of these samples highly enriched in deuterium give rise to some difficulties. Common isotope ratio mass spectrometers are not designed to analyze waters with such peculiar isotope compositions. In order to avoid possible analytical inaccuracies from the mass spectrometer (mainly produced by poor linearity) or from the preparative method, and to make adequate corrections and normalization, four standards were prepared from commercial deuterium oxide enriched to 99.9% in deuterium (Cambridge Isotope Laboratories, Inc). The selected dilutions for the standards were 1:50 (1.998 % D), 1:200 (0.4995 % D, 1:500 (0.1998 % D) and 1:1000 (0.0999 % D). A considerable number of standards were processed together with the samples and their results were employed to correct the isotope composition of the water samples by linear correlation. The standard deviation in the determination of the δD value was 1%.

The hydrogen for the isotope ratio analysis was extracted from the water by reduction with zinc (provided by Indiana University). In this process, 8 microliters of water are added to "Ace Glass" stopcocks containing 0.5 g of Zn. The mixture is frozen at liquid nitrogen temperature and a vacuum is applied through a diffusion pump. Then, the stopcocks are heated in an aluminum furnace during 90 minutes at 475 ºC. After cooling, the stopcock is connected to the manifold of a dual inlet "VG Prism II" Isotope Ratio Mass Spectrometer.

Iodide was determined by using two analytical techniques; the potentiometric method (also called Ion Selective Electrode) and ion chromatography. In the first method, an Orion Model 94-53 iodide electrode, together with a simple-junction Orion 90-01 reference electrode and an Orion Model 901 microprocessor ion analyzer, were used. The electrode potential of standard solutions was measured to determine the calibration curve in two concentration intervals. The direct measurement procedure was used in all linear regions. The detection limit was 10 $\mu g \cdot l^{-1}$. Iodide was also quantified by the ion chromatography technique using a Dionex 4500i ion chromatograph. The analytical columns included a guard column Dionex AG9 and a separator column Dionex AS9. Detection was achieved with a conductivity detector. A Dionex Anion Micromembrane Suppressor AMMS-II was used in order to suppress the conductivity of the eluent. The calibration standard was prepared daily by dilution of a 1000 $mg \cdot L^{-1}$ stock solution (1.18 g reagent-grade NaI in a 1 l volumetric flask). The detection limit for a 25 µl injection volume was 0.11 $mg \cdot l^{-1}$ (calibration curve in the range 1-25 $mg \cdot l^{-1}$) and for a 100 µl injection volume was 10 $\mu g \cdot l^{-1}$ (calibration curve in the range 25-1000 $\mu g \cdot l^{-1}$).

Lithium and rubidium. Total Li was analyzed by flame photometry using a Perkin Elmer 2280 atomic absorption spectrophotometer, measuring the lithium emission at 670.6 nm. Due to the low Li concentrations observed in the pore water samples, calibration standards ranging from 0.01 to 1.0 $mg \cdot l^{-1}$ of Li were prepared. The quantification limit, according to Eurachem recommendations, was 0.01 $mg \cdot l^{-1}$. Reproducibility was close to 5% at concentrations close to the quantification limit and below 1% at concentrations above 0.1 $mg \cdot l^{-1}$. The method was validated against a water sample containing 0.02738 $mg \cdot l^{-1}$ of Li prepared by the U.S. Geological Survey and the National Institute for Science and Technology and certified by the JRC-IRMM during the IMEP-9 programme.

The total Rb content was determined by inductively coupled plasma mass spectrometry (ICP-MS), using a Finnigan MAT SOLA instrument equipped with a quadrupole analyzer and both Faraday cup and continuous dynode electron multiplier. The measurements were performed using external calibration and Ga as internal standard. Final concentration was calculated taking into account the $^{85}Rb/^{87}Rb$ isotopic ratio for each sample. Detection limit was below 0.2 $\mu g \cdot l^{-1}$ and reproducibility was close to 2%.

The isotopic analysis of Li and Rb was performed in two steps: (i) purification and separation of Li and Rb from the sample matrix using a cation exchange resin, and (ii) measurement of $^{6}Li/^{7}Li$ and $^{85}Rb/^{87}Rb$ isotopic ratio by thermal ionization mass spectrometry (TIMS). The whole procedure is summarized in the flow chart given in the Fig. 3 and the experimental details are given below.

Ion exchange chromatography. The purification and separation procedure developed in this study is an optimized combination of several chromatographic methods used for the separation of Li and Rb from geological samples (Sanz and Wasserburg, 1969; You and Chan, 1996; Moriguti and Nakamura, 1998). PTFE columns with a PTFE mesh plug as support of the resin bed were filled up with Dowex resin (50W-X8, 200-400 mesh). Then, the resin was cleaned with H_2O and 6 M HCl and finally conditioned with 2.5 M HCl. The whole separation process was performed using 2.5 M HCl as eluent. 1 ml of the aqueous sample was evaporated to dryness and the residue was dissolved in 2 ml of 2.5 M HCl. This solution was loaded onto the resin bed, which was then rinsed with 5 ml of the eluent. The Li fraction was subsequently eluted with 4 ml of the 2.5 M HCl. After that, 13 ml of 2.5 M HCl were passed through the column to eliminate Na, prior to the Rb collection with 7 ml of the acid eluent. The separated Li and Rb fractions were then evaporated to dryness under infrared light. The residues were finally dissolved with the appropriate H_2O volume, according to the element concentration previously determined.

Mass spectrometry. The samples were analyzed in a 60º magnetic sector NIST mass spectrometer, fitted with a Faraday collector. The source and the collector slit openings were 0.007 and 0.04 inches, respectively, for both elements. The accelerating voltage was set at 9780 V. The source configuration was triple rhenium filament for Li and single rhenium filament with the silica gel technique for Rb. The measurements were performed using a program developed in the laboratory based on LabView 7.0 software. When the isotope ratios were calculated, a linear interpolation was applied in order to correct for possible variations in signal intensity during the measurement. The instrumental mass discrimination factors were checked against the standards SRM-987 and IRMM-016a for Rb and Li, respectively. The typical internal reproducibility was below 0.5% (average of 10 ratios) for both elements and is expressed as 1 standard deviation.

Results and interpretation

The results of the diffusion experiment included the evolution of tracer concentrations in the injection system and tracer distribution profiles in the rock. Two and three-dimensional modeling of the results has been performed using the CRUNCH (Steefel, 2006) and CORE^{3D} (Yang et al., 2003) reactive transport codes, respectively.

Modeling with CRUNCH

The results from the field experiment have been interpreted by means of two-dimensional transport calculations including diffusion and sorption. The experiment was designed so the length of the injection interval was larger than tracer transport distances. This experimental setup favors, in principle, a simple 2D interpretation of the results, since diffusion occurs mainly along bedding planes.

The finite difference reactive transport code CRUNCH has been used for the simulations. CRUNCH is the latest evolution of the GIMRT/OS3D software package (Steefel, 2001; Steefel and Yabusaki, 1996).

The equation of conservation of mass for a given tracer can be written as

$$\frac{\partial c_{tot}}{\partial t} = \nabla \cdot (D_e \nabla c) \qquad (1)$$

where c is concentration in solution [moles per volume of solution], t is time [s], D_e is the effective diffusion coefficient [$m^2\ s^{-1}$], ϕ is the accessible porosity for the tracer and c_{tot} is the total concentration of tracer [moles per bulk volume], which is given by

$$c_{tot} = \phi c + \rho_d s \tag{2}$$

where ρ_d is the bulk dry density [kg m^{-3}] and s is the concentration of tracer sorbed on the solids [moles per mass of solid]. Linear sorption ($s = K_d c$) has been assumed for the sorbing tracers. With the inclusion of linear sorption, the total concentration c_{tot} can also be expressed as the product of a rock capacity factor α and the concentration in solution c ($c_{tot} = \alpha c = (\phi + \rho_d K_d)\ c$).

The geometry of the problem is schematically shown in Fig. 4. The calculation domain corresponds to a bedding plane. The fact that the bedding is at an angle (58º) with respect to the borehole is taken into account by the elliptical shape of the borehole (intersection of bedding and borehole). The dip of bedding is 32º. All the boundaries of the domain are no-flux boundaries. The initial conditions are

Borehole: $c(x,y,t=0) = c_{tot}(x,y,t=0) = c_0$

Rock: $c_{tot}(x,y,t=0) = c_{back}$

where c_0 is the initial concentration in the injection system and c_{back} is the background concentration of the tracer in the Opalinus Clay. Only a quarter of the two-dimensional system is taken into account in the calculations due to symmetry considerations (diffusion is assumed to be homogeneous and isotropic along the plane). A large value of D_e is assumed in the borehole, in order to maintain a homogeneous concentration (well mixed conditions in the injection system). The total volume of solution in the injection system (about 30 l) is also taken into account.

The results of model calculations are compared with the evolution of tracer concentrations in the injection system and the measured tracer profiles in the rock around the borehole. In the case of the tracer profiles not measured along a bedding plane it has been necessary to project those profiles onto the bedding plane, in order to be able to compare them with the results of the 2D model calculations. Profile 12, at the bottom of the borehole, was not

included in any of the results for the 2D calculations. Fitting tracer concentrations in (a) the injection system and (b) in the rock profiles provides a unique set of effective diffusion coefficients (D_e) and porosity/sorption values (rock capacity factors in the case of linear sorption).

HDO is a non-sorbing tracer and is used to measure the transport properties of water. The best agreement between model calculations and experimental results was obtained using D_e = 5.0x10^{-11} m^2/s and ϕ = 0.16 (Fig. 5). The obtained value of porosity is identical to the measured average water content porosity. These values are similar to the parameters obtained from laboratory through-diffusion experiments parallel to bedding at 23ºC and also to the results of the DI-A in-situ diffusion experiment (Table 1). Notice that at very early times, concentrations in the circulation tank show a very large dispersion of values possibly due to incomplete mixing of the tracer at the time of the sampling. Also, this fit was obtained using a value of the initial concentration c_0 equal to 0.125 (12.5% deuterium), instead of the theoretical value of 0.132, which was based on the volume of synthetic solution in the circulation system and the mass of tracer added to the system. Background concentration in the rock porewater was assumed to be equal to 10^{-4} (0.01% deuterium), based on the natural abundance of deuterium.

Regarding the tracer profiles in the rock, one of the profiles (profile 11) shows distinctively lower concentrations than the rest of the profiles. This effect may be due to the fact that profile 11 is in the uppermost part of the overcore and pointing upwards (Fig. 2). This profile may capture the curvature of the tracer plume near this end of the interval, which cannot be reproduced by the 2D model. However, the effect of the natural heterogeneity of the rock cannot be ruled out, as discussed below.

The error in the fitting procedure for HDO has been estimated to be about 40% for D_e and 20% for ϕ, based on the sensitivity of model results to changes in the values of the parameters.

Iodide was assumed to be non-sorbing. The best agreement between model calculations and experimental results was obtained using D_e = 1.2x10^{-11} m^2/s and ϕ = 0.09 (Fig. 6). These values are in good agreement with the results for Cl^-, Br^- and I^- from through-diffusion experiments at 23ºC (Table 1). Comparison with the results from the DI-A in-situ diffusion coefficient shows also similar values. Notice that at very early times, concentrations in the circulation tank show a very large dispersion of values possibly due to incomplete mixing of the tracer at the time of the sampling. Also, this fit was obtained using a value of the initial

concentration c_0 equal to 1.52×10^{-2} mol/l, instead of the theoretical value of 1.58×10^{-2} mol/l, which was based on the volume of synthetic solution in the circulation system and the mass of tracer added to the system. Background concentration in the rock was assumed to be equal to 10^{-5} mol/l, based on the composition of porewaters sampled in the vicinity of the test borehole (Pearson et al., 2003).

Two different sets of iodide profiles can be observed in Fig. 6b. First, iodide concentrations in the pore water are calculated from the experimental data using the measured water content, i.e., the total water-filled porosity. The average water-content porosity of the analyzed samples is 0.164 (standard deviation = 0.02). Dividing the tracer concentrations in the profiles by a factor of 0.53, a good agreement between model and experimental results is achieved. This factor of 0.53 is equivalent to assuming that only 53% of the water-content porosity is accessible to iodide, i.e., the average accessible porosity for iodide is 0.09. This is the value used in the model calculations.

Regarding the tracer profiles in the rock, one of the profiles (profile 11, same as for HDO) shows distinctively lower concentrations than the rest of the profiles. This effect may be due to the fact that profile 11 is in the uppermost part of the overcore and pointing upwards (Fig. 2). This profile may capture the curvature of the tracer plume near this end of the interval, which cannot be reproduced by the 2D model. However, the effect of the natural heterogeneity of the rock cannot be ruled out, as discussed below.

The error in the fitting procedure for I^- has been estimated to be about 20% for both D_e and ϕ, based on the sensitivity of model results to changes in the values of the parameters.

$^6Li^+$ was used as a stable isotope tracer. In principle, it was assumed that it should behave as a conservative or very weakly sorbing tracer. The best agreement between model calculations and experimental results was obtained using $D_e = 7 \times 10^{-11}$ m^2/s and a rock capacity factor $\alpha = 0.70$ ($\phi = 0.164$, $K_d = 0.24$ l/kg, Fig. 7). These values are similar to the parameters obtained from laboratory through-diffusion experiments parallel to bedding at 23ºC for Na^+ ($D_e = 7.2 \pm 0.5 \times 10^{-11}$ m^2/s, $\alpha = 0.62 \pm 0.05$, Van Loon et al., 2004a). Clearly, $^6Li^+$ did not behave as a conservative tracer. As it occurred with the other tracers, concentrations in the circulation tank at very early times show a very large dispersion of values possibly due to incomplete mixing of the tracer at the time of the sampling. Also, this fit was obtained using a value of the initial concentration c_0 equal to 0.19 mg/l (3.16×10^{-5} mol/l) instead of the theoretical value of 0.202 mg/l (3.36×10^{-5} mol/l), which was based on the volume of synthetic solution in the circulation

system and the mass of tracer added to the system. Total (sorbed + solution) background concentration in the rock was assumed to be equal to 0.1 mg/l (0.023 mg/l in the porewater), based on the composition of porewaters sampled in the vicinity of the test borehole (Pearson et al., 2003), the natural abundance of ^{6}Li relative to total Li ($^{6}Li/(^{6}Li+^{7}Li)=0.075$), and the value of K_d used in the calculation.

Regarding the tracer profiles in the rock, one of the profiles (profile 11) shows distinctively higher concentrations than the rest of the profiles. This effect cannot only be due due to the fact that profile 11 is in the uppermost part of the overcore and pointing upwards (Fig. 2). It is probable that profile 11 also reflects the natural heterogeneity of the rock.

The error in the fitting procedure for $^{6}Li^{+}$ has been estimated to be about 30% for both D_e and α, based on the sensitivity of model results to changes in the values of the parameters.

$^{87}Rb^{+}$ was used as a stable isotope tracer subject to relatively strong sorption. Due to the variability displayed between the different measured profiles in the rock it has not been possible to assign a unique value of D_e and α to this tracer. Figure 8 shows two sets of results corresponding to two possible average sets of values for the diffusion and sorption parameters. In one case (Fig. 8a,b) the values of the effective diffusion coefficient and rock capacity factor are $D_e = 5\text{x}10^{-11}$ m^2/s and $\alpha = 20$ ($\phi = 0.164$, $K_d = 8.8$ l/kg), and an initial concentration c_0 equal to $2.1\text{x}10^{-5}$ g/l ($2.4\text{x}10^{-7}$ mol/l) was used instead of the theoretical value of $2.783\text{x}10^{-5}$ g/l ($3.2\text{x}10^{-7}$ mol/l), which was based on the volume of synthetic solution in the circulation system and the mass of tracer added to the system. In the other case (Fig 7a,b) the values of the effective diffusion coefficient and rock capacity factor are $D_e = 10^{-10}$ m^2/s and $\alpha = 80$ ($\phi = 0.164$, $K_d = 35.4$ l/kg), and the theoretical concentration c_0 equal to $2.783\text{x}10^{-5}$ g/l ($3.2\text{x}10^{-7}$ mol/l) was used. The large variability in the profiles for strongly sorbing tracers has also been observed for Cs^{+} and Co^{2+} in the DI-A and DI-A2 experiments at Mont Terri (Van Loon et al., 2004b; Wersin et al., 2006; Wersin et al., 2007). This variability seems to reflect the natural small-scale heterogeneity of the Opalinus Clay regarding sorption properties.

Modeling with CORE^{3D}

A fully 3D anisotropic finite element model of the DI-B experiment has been used for the interpretation of in situ experiments. Tracer diffusion plumes are symmetric with respect to a vertical plane perpendicular to bedding which divides vertically the borehole into two equal parts. Therefore, only half of the system needs to be modeled. The model domain was

discretized using hexahedral finite elements which are small near the borehole and increase their size far away from the borehole.

The numerical model considers three material zones: (1) the packed-off section of the borehole where tracers are injected; (2) the steel plate at the bottom of the borehole with a thickness of 1 cm and (3) the Opalinus clay. In the model the borehole has a porosity equal to 1 and a sufficiently large diffusion coefficient to ensure a homogenous tracer distribution within the borehole. Small values of porosity and an extremely small effective diffusion coefficient are adopted for the steel plate at the bottom of the borehole. Parameters of the Opalinus Clay are tracer-dependent. The numerical model considers the angle between bedding and the x–y horizontal plane to be 32º. Background tracer concentrations are much smaller than measured concentrations along profiles. Therefore, it can be assumed that initial tracer concentrations in the clay are equal to zero. Tracers diffuse from the borehole into the Opalinus clay. All external boundaries of the model are no-flow boundaries.

The transport equation for a tracer which diffuses into a very low permeability medium is given by (Bear, 1972)

$$\phi R \frac{\partial c}{\partial t} = \nabla \cdot \left(\overline{D}_e \nabla c \right) \tag{3}$$

where c is tracer concentration, t is time, ϕ is accessible porosity, which accounts also for anion exclusion, and R is the retardation factor ($R = 1 + \rho_d K_d / \phi$). For a conservative tracer, R is equal to 1 and ϕ is equal to the total porosity if the tracer is not affected by anion exclusion. $\overline{D}_e$ is the effective diffusion tensor given by

$$\overline{D}_e = \begin{pmatrix} D_{xx} & D_{xy} & D_{xz} \\ D_{yx} & D_{yy} & D_{yz} \\ D_{zx} & D_{zy} & D_{zz} \end{pmatrix} \tag{4}$$

which can be diagonalized as

$$\overline{D}_e = \begin{pmatrix} D_{\xi\xi} & 0 & 0 \\ 0 & D_{\eta\eta} & 0 \\ 0 & 0 & D_{\varsigma\varsigma} \end{pmatrix} \tag{5}$$

where $D_{\xi\xi}$, $D_{\eta\eta}$ and $D_{\zeta\zeta}$ are the principal components of the diffusion tensor. The components of the effective diffusion tensor in (4) can be calculated from the main components in (5) using equations similar to those of the permeability tensor (Bear, 1972).

CORE^{3D} (Yang et al., 2003) has been used to simulate the DI-B in situ experiment. CORE^{3D} is a fully three-dimensional computer code for modeling saturated water flow, heat transport and multi-component reactive solute transport under both local chemical equilibrium and kinetic conditions and its capability to simulate 3D anisotropic diffusion has been verified with analytical solutions.

HDO and iodide. Model parameters were calibrated with deuterium and iodide measured concentrations in the borehole and along profiles (Fig. 9). Calibrated values for deuterium diffusion parameters are $4x10^{-11}$ m/s^2 and 10^{-11} m/s^2 for the effective diffusion coefficients parallel ($De_{\|}$) and perpendicular ($De_{\perp}$) to bedding, respectively, and 0.15 for total porosity. In the case of iodide, the calibrated effective diffusion coefficient parallel to bedding is $8.3x10^{-12}$ m/s^2 with an anisotropy ratio of 4, and the calibrated value for porosity is 0.08. For both tracers, the value of the anisotropy ratio $De_{\|}/De_{\perp} = 4$ is based on the results of small-scale laboratory experiments (Van Loon et al., 2004a).

Comparison of computed and measured concentrations for HDO and I^- has been already presented in Samper et al. (2006, 2007). The numerical model reproduces the overall trend for measured data in the borehole and along profiles. However, computed profiles 10 and 11 slightly overestimate measured data. Sensitivity analysis performed to evaluate uncertainties (Samper et al., 2006, 2007) shows that is not possible to improve fit of profiles 10 and 11 by varying diffusion parameter values without spoiling fit of the other computed profiles to measured data. Variation of anisotropy ratio in the range of values obtained in the laboratory does not imply significant variations in computed profiles and therefore, does not improve the fit of profiles 10 and 11 to experimental data. On the other hand, influence of anisotropy ratio variation increases proportional to angle between bedding plane and profile. Experimental errors during measurement or variation of bedding angle with depth might lead to error in the value of this angle. Thus, a sensitivity analysis to bedding angle and to angle between profiles and bedding has been performed for both tracers in order to achieve a simultaneous fit of all the profiles (Fig. 10).

Sensitivity of dilution inside borehole to a variation of bedding angle that can be caused by experimental errors is negligible. Computed profiles sensitivity depends on profile direction and increases with distance to axis. Profiles parallel to bedding are not sensitive to bedding

angle variation but the rest of profiles are. Increase of bedding angle leads to a better fit of profiles 10 and 11 but implies underestimation of profiles 6, 7 and 8.

Fixing the bedding angle value, uncertainty in the measured orientation of profiles 10 and 11 has been evaluated by means of a sensitivity analysis of computed concentrations to variation of angle between profile direction and bedding plane (Fig. 11). Reference value of angle is 74º for both profiles. The fit of computed profiles to measured data improves when the angle decreases. An angle of 54º, which would be equivalent to a 20º experimental error, leads to an excellent fit of profile 10 for both tracers. In the case of profile 11, computed profiles overestimate measured data for any feasible angle value. This is probably due to the existence of heterogeneities in the rock.

$^{6}Li^{+}$ and $^{87}Rb^{+}$ measured concentrations along profiles present strong fluctuations (Figs. 12, 13). Thus, calibration of diffusion parameters has been performed from available dilution data (tracer concentrations in the circulation system). Accessible porosity and anisotropy ratio were fixed and assumed to be equal to those of HDO. The best fit of computed dilution curve to measured data for $^{6}Li^{+}$ was achieved for D_e= 7.07x10^{-11} m^2/s and K_d = 0.2 l/kg. In the case of $^{87}Rb^{+}$, the best fit was achieved for D_e= 1.41x10^{-10} m^2/s and K_d = 10 l/kg, although subject to a very significant uncertainty.

Comparison of the results

Table 1 shows a summary of the results from this study (interpretation of the experimental data using CRUNCH and CORE^{3D}), and a comparison with results from other in-situ and small-scale laboratory experiments.

Inspection of the results reveals that the parameters obtained for HDO and iodide agree well with the results from the other experiments and their range of variability. Anion exclusion clearly affects iodide, which displays effective diffusion coefficients and accessible porosities smaller than those for water (HDO, HTO).

Regarding $^{6}Li^{+}$, it had been expected that it would behave in a conservative or very weakly-sorbing manner. However, the parameters obtained for this tracer agree well with those obtained for Na^{+} in other studies. Na^{+} behaves in the Opalinus Clay as a weakly sorbing element. Na^{+} is the major cation in the Opalinus Clay porewater, with a porewater concentration of about 2.5 mol/kg_H2O in the vicinity of the DI niche (Pearson et al., 2003), where the different in-situ experiments have been performed.

The measured $^{87}Rb^{+}$ profiles show a large variability. Also, the shape of the tracer evolution curve in the circulation system is rather irregular (Figs. 8, 13). These experimental

results do not allow the determination of a unique set of transport (D_e) and sorption (K_d) parameters. However, strong sorption of $^{87}Rb^+$ has been confirmed. The large variability of tracer profiles in the rock has also been observed for other strongly sorbing tracers (Cs^+, Co^{2+}) in the DI-A1 and DI-A2 in-situ diffusion experiments (Van Loon et al., 2004b; Wersin et al., 2006, 2007). This variability suggests that the small-scale heterogeneity associated with the mineralogy of the rock plays an important role in the distribution of tracers with strong affinities for mineral surfaces.

Conclusions

The DI-B experiment was a Spanish Project led by Enresa. One of its main objectives was to study the transport and retention properties of selected tracers in the Opalinus Clay, but using only non radioactive species. The selected tracers were HDO (water), I^- (anionic species), $^6Li^+$ (non- or weakly-sorbing cation) and $^{87}Rb^+$ (strongly-sorbing cation).

The experimental results were modeled using two different reactive transport codes and spatial geometries (CRUNCH (2D) and CORE^{3D}). The results for HDO and iodide from both approaches showed good consistency and compare well with the results from other in-situ tests and small-scale laboratory experiments. The effect of anion exclusion on the behavior of iodide has been confirmed. $^6Li^+$ has been shown to behave as a weakly sorbing tracer, with effective diffusion coefficients (D_e) and sorption parameters (K_d) very similar to those of Na^+. Tracer profiles for $^{87}Rb^+$ showed a large degree of variability and it was not possible to assign unique values of D_e and K_d. This variability has also been observed for other strongly sorbing tracers in the DI-A1 and DI-A2 in-situ diffusion tests, and it may be related to the small-scale mineralogical heterogeneity of the rock.

A larger scale heterogeneity has also been observed. One of the measured tracer profiles (profile 11) displays anomalous tracer concentrations when compared with the other measured profiles. A sensitivity analysis concerning geometrical aspects has confirmed that this anomalous profile is the result of a natural heterogeneity of the rock.

Table 1. Effective diffusion coefficientes (D_e, parallel to bedding), porosities (ϕ) and distribution coefficients (K_d) from this study (DI-B), other in-situ diffusion experiments at Mont Terri (DI-A1, DI-A2), and small scale laboratory through-diffusion experiments.

Tracer	Parameter D_e (m^2/s) ϕ K_d (l/kg)	In-situ test DI-B CRUNCH (2D)	In-situ test DI-B $CORE^{3D}$	In-situ test DI-A1 [a] CRUNCH (2D)	In-situ test DI-A2 [b] CRUNCH (2D)	Lab data diffusion || bedding
HDO	D_e ($x10^{-11}$)	5.0	4.0	5.4	6.0	5.4 (HTO) [c], 4.0 (HTO) [d]
	ϕ	0.16	0.15	0.18	0.15	0.15-0.17 (HTO) [c]
I^-	D_e ($x10^{-11}$)	1.2	0.83	1.3	3.0	1.4 (I^-) [d,e], 1.6 (Cl^-) [c], 1.5 (Br^-) [e]
	ϕ	0.09	0.08	0.09	0.08	0.12 (I^-) [e], 0.08 (Cl^-) [c], 0.09 (Br^-) [e]
$^6Li^+$	D_e ($x10^{-11}$)	7.0	7.1	7.2 (Na^+)		7.2 (Na^+) [c]
	ϕ	0.16	0.15	0.18 (Na^+)		0.15 – 0.17 (HTO) [c]
	K_d	0.24	0.20	0.20 (Na^+)		0.20 (Na^+) [c]
$^{87}Rb^+$	D_e ($x10^{-11}$)	5 - 10	14.1			
	ϕ	0.16	0.15			
	K_d	9 - 36	10			

a) Van Loon et al. (2004b), Wersin et al. (2006)
b) Wersin et al. (2007)
c) Van Loon et al. (2004a)
d) Yllera et al. (2004)
e) unpublished results from Paul Scherrer Institut

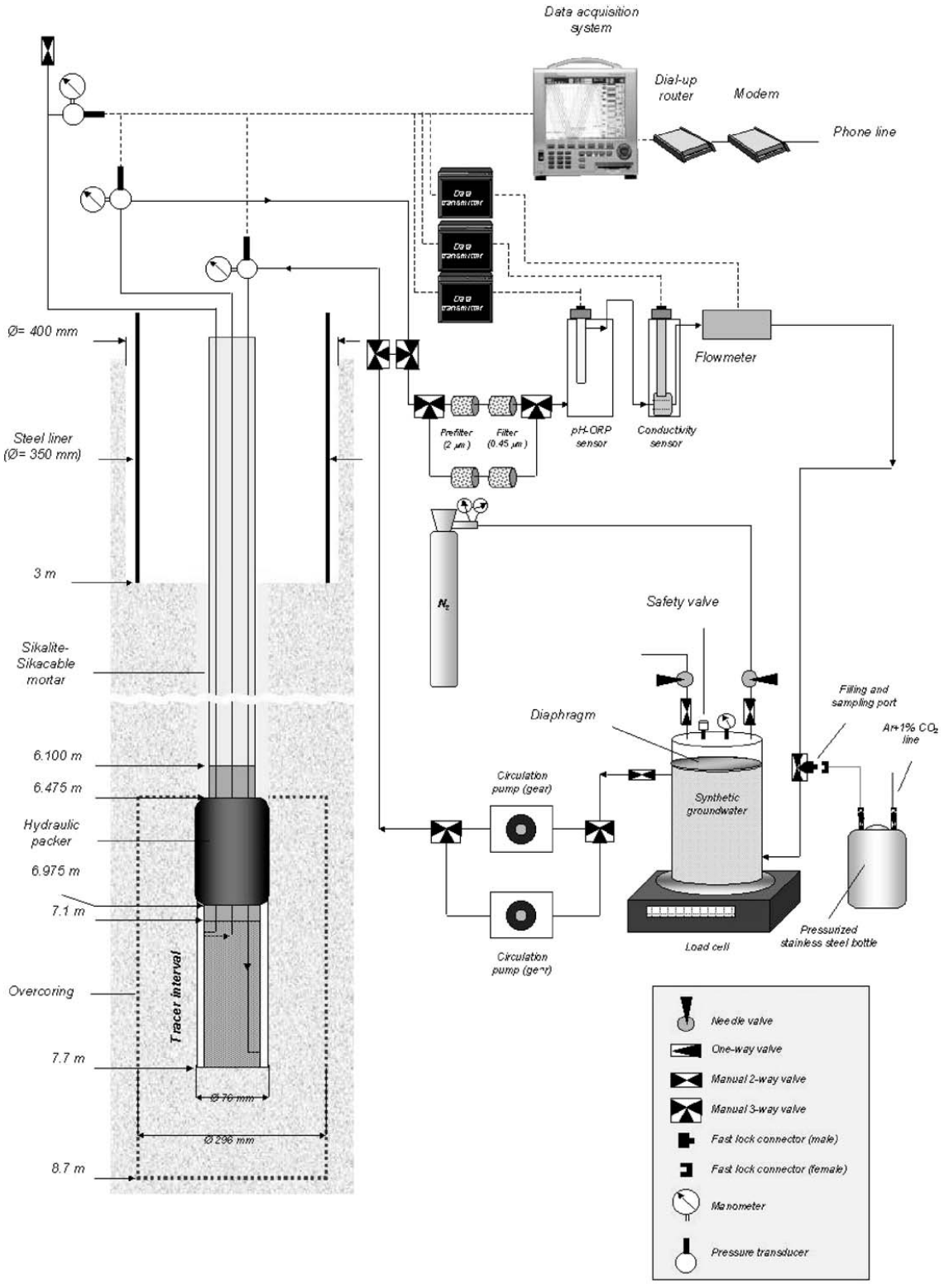

Fig.1. Experimental setup of the DI-B in-situ diffusion experiment. Downhole (left) and surface (right) instrumentation. After Yllera et al. (2004).

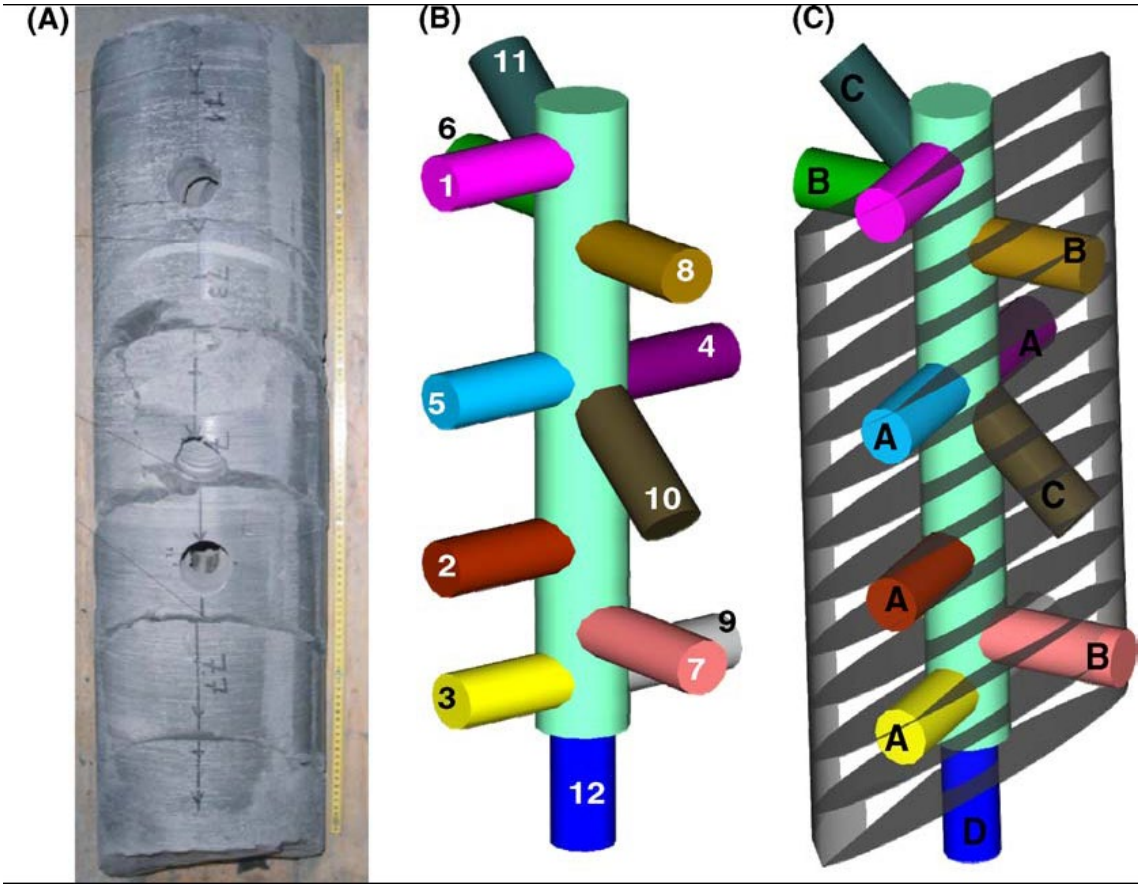

Fig. 2. (A) View of overcore of BDI-B3, (B) schematic location of the 12 sampling profiles and (C) types of profiles depending on their orientation with respect to bedding. After Samper et al. (2006).

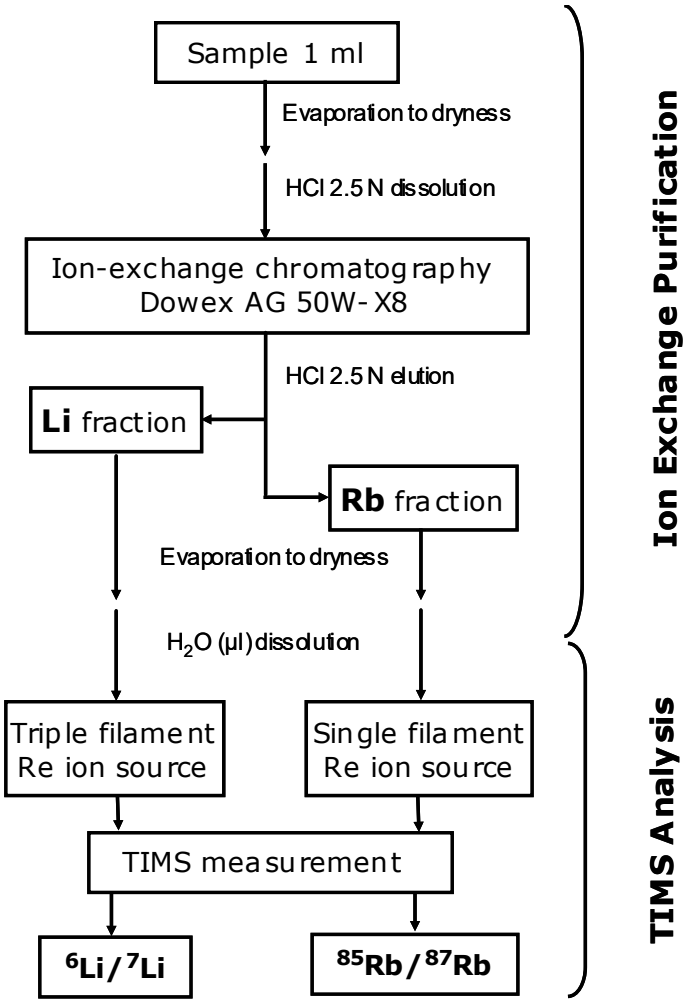

Fig. 3. Protocol for the purification and isotopic analysis of the Li and Rb tracers.

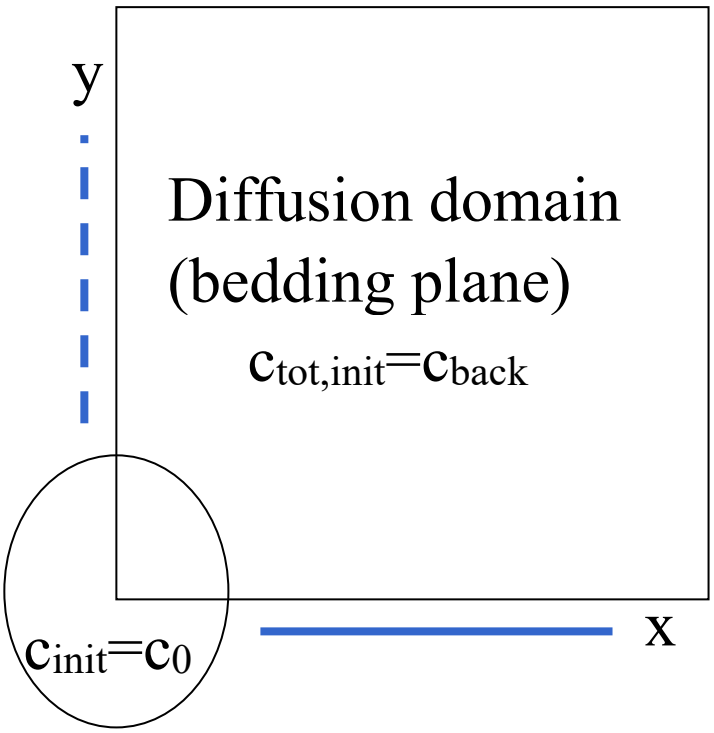

Fig. 4. Schematic representation of the geometry of the model. The calculation domain corresponds to a bedding plane and the borehole (area enclosed by the square). The trace of the borehole is not cylindrical due to the 58º angle between bedding and borehole. The solid and dashed lines parallel to the x and y axes make reference to the orientations of the calculated tracer profiles shown in the Figs. that follow.

(a)

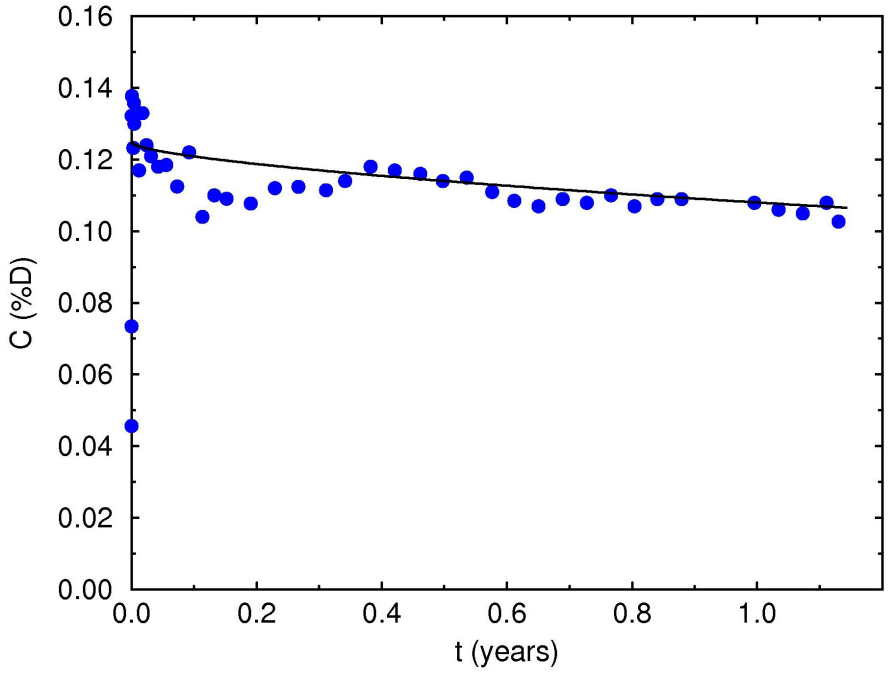

(b)

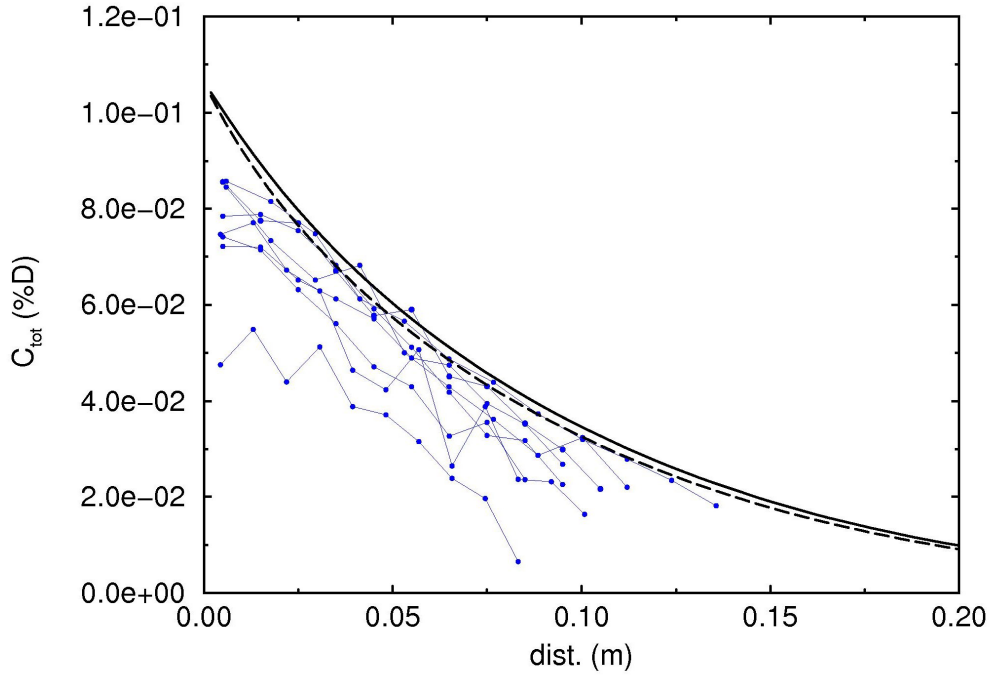

Fig. 5. Results for HDO. Model parameters: D_e=5.0x10^{-11} m^2/s, ϕ=0.16. (a) Concentration in the injection system vs. time. The dots are experimental data; the line represents model calculations. (b) Tracer profiles in the rock (total concentration vs. distance from borehole wall). Thick lines correspond to model results; thin lines correspond to experimental data. All concentrations are in units of atom% of deuterium in the water.

(a)

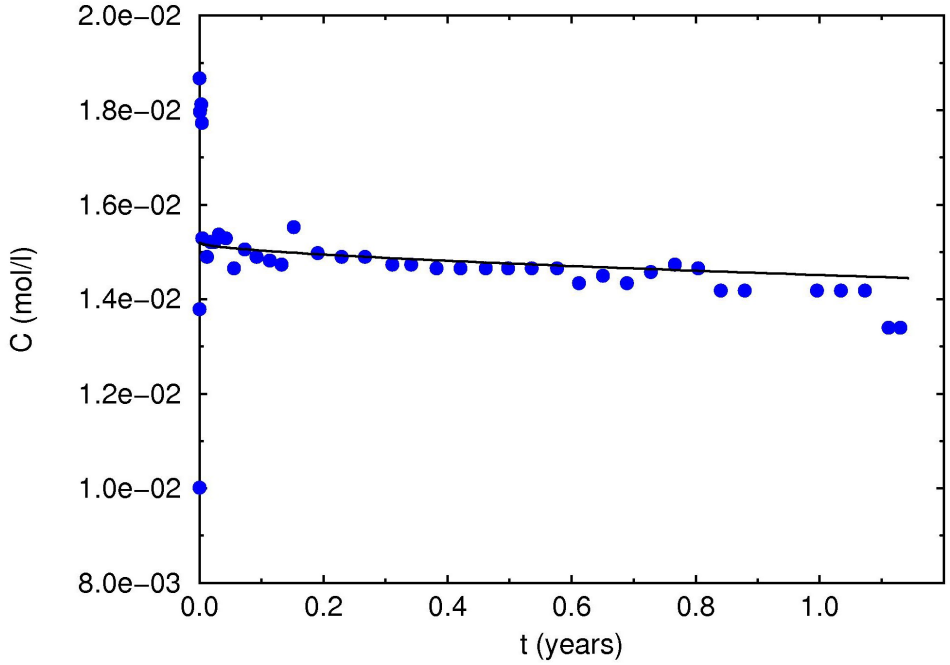

(b)

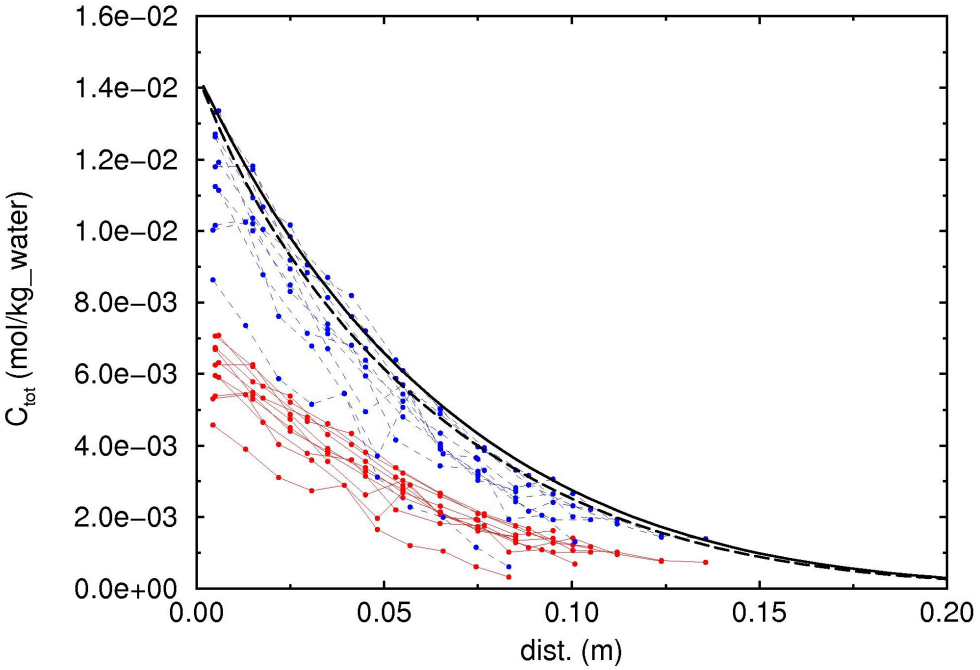

Fig. 6. Results for I^-. Model parameters: D_e=1.2x10^{-11} m^2/s, ϕ=0.09. (a) Concentration in the injection system vs. time. The dots are experimental data; the line represents model calculations. (b) Tracer profiles in the rock (total concentration vs. distance from borehole wall). Thick lines correspond to model results; thin lines correspond to experimental data. Two sets of profiles, calculated with different water contents, are shown (see text for explanation).

(a)

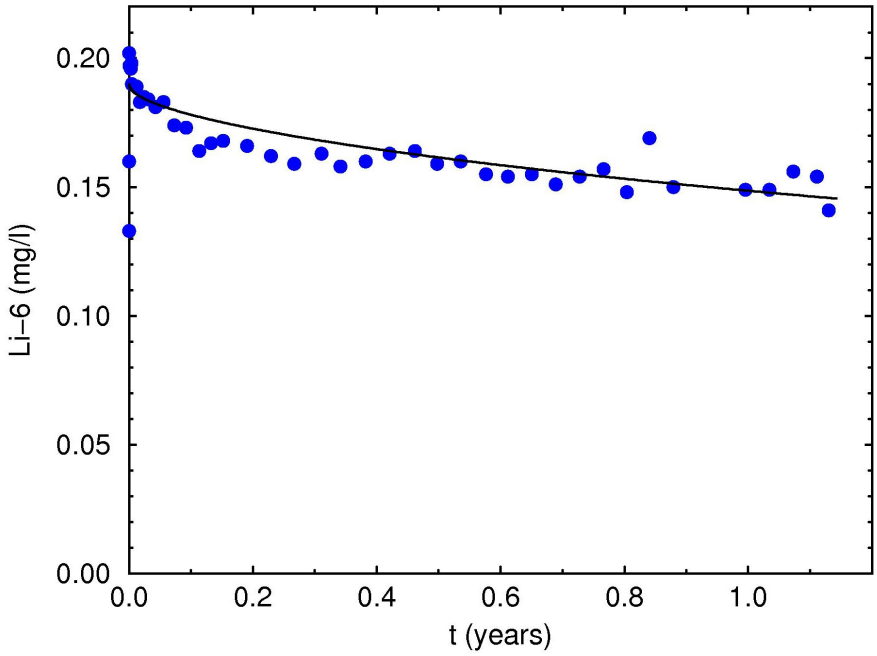

(b)

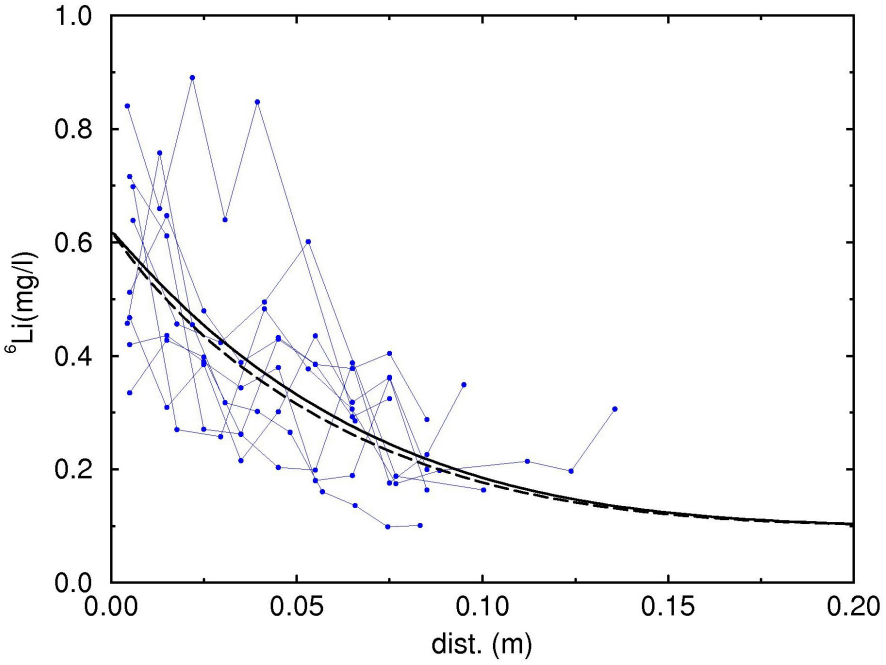

Fig. 7. Results for $^6Li^+$. Model parameters: D_e=7.0x10^{-11} m^2/s, α=0.70 (ϕ=0.164, K_d=0.24 l/kg). (a) Concentration in the injection system vs. time. The dots are experimental data; the line represents model calculations. (b) Tracer profiles in the rock (total concentration vs. distance from borehole wall). Thick lines correspond to model results; thin lines correspond to experimental data. Notice that in the rock profiles, concentrations correspond to the sum of sorbed concentrations and concentrations in solution.

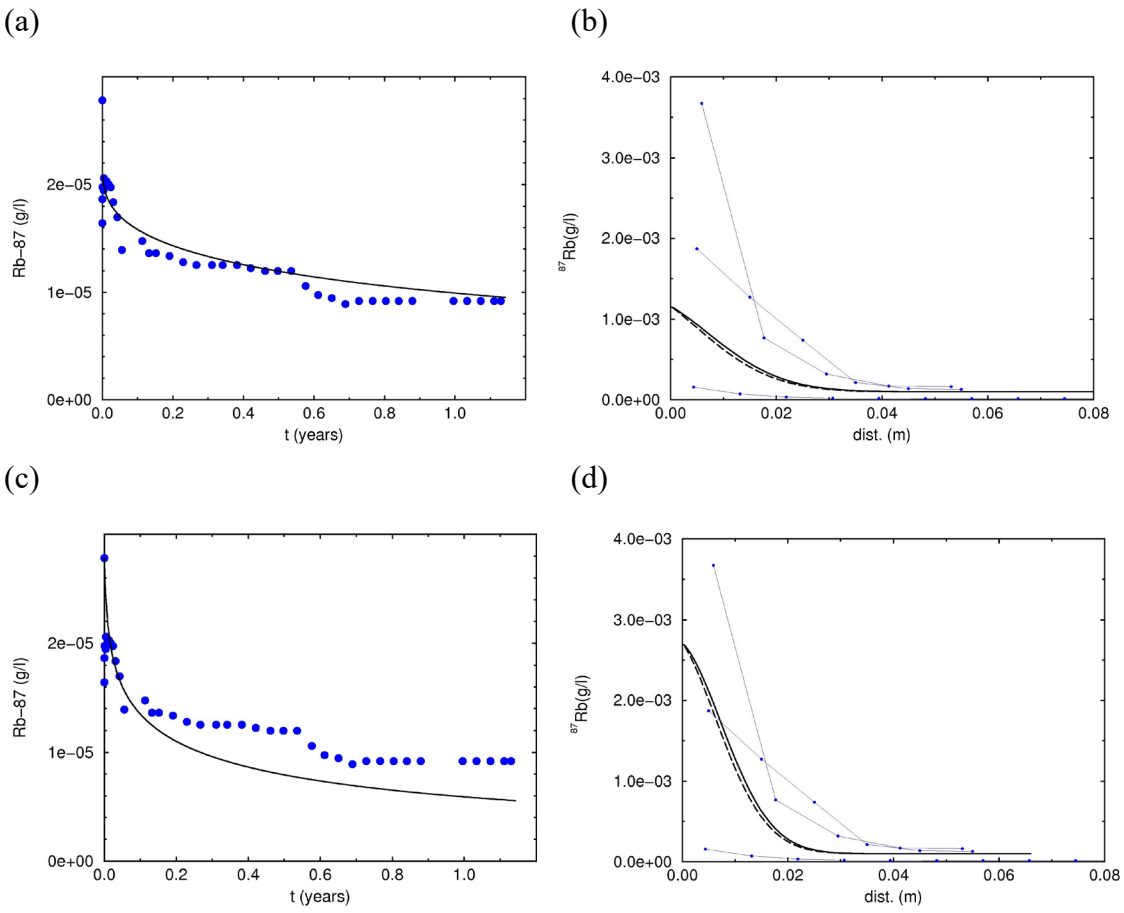

Fig. 8. Results for $^{87}Rb^{+}$. Model parameters (a,b): D_e=5.0x10^{-11} m^2/s, α=20 (ϕ=0.164, K_d=8.8 l/kg). Model parameters (c,d): D_e=10^{-10} m^2/s, α=80 (ϕ=0.164, K_d=35.4 l/kg). (a,c) Concentration in the injection system vs. time. The dots are experimental data; the line represents model calculations. (b,d) Tracer profiles in the rock (total concentration vs. distance from borehole wall). Thick lines correspond to model results; thin lines correspond to experimental data. Notice that in the rock profiles, concentrations correspond to the sum of sorbed concentrations and concentrations in solution.

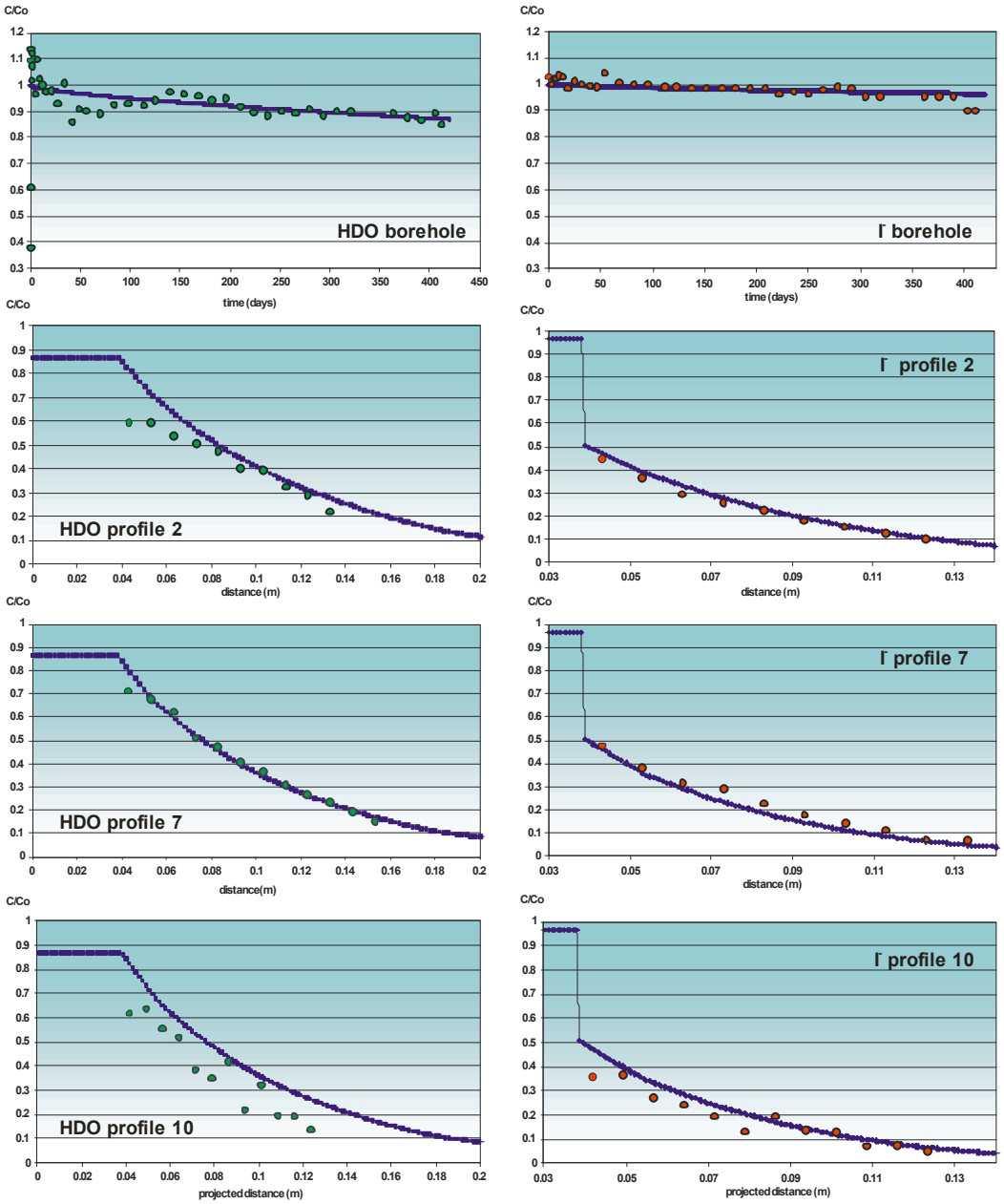

Fig. 9. Fit of HDO and iodide computed concentrations to measured data in the borehole and along different profiles of at the end of the experiment. All concentrations are relative concentrations in solution (C/C_0). Distance is with respect to borehole axis (borehole radius = 0.038 m). The sudden drop of I^- concentrations in the profiles at the borehole wall reflects the correction applied to the calculated values to account for anion exclusion.

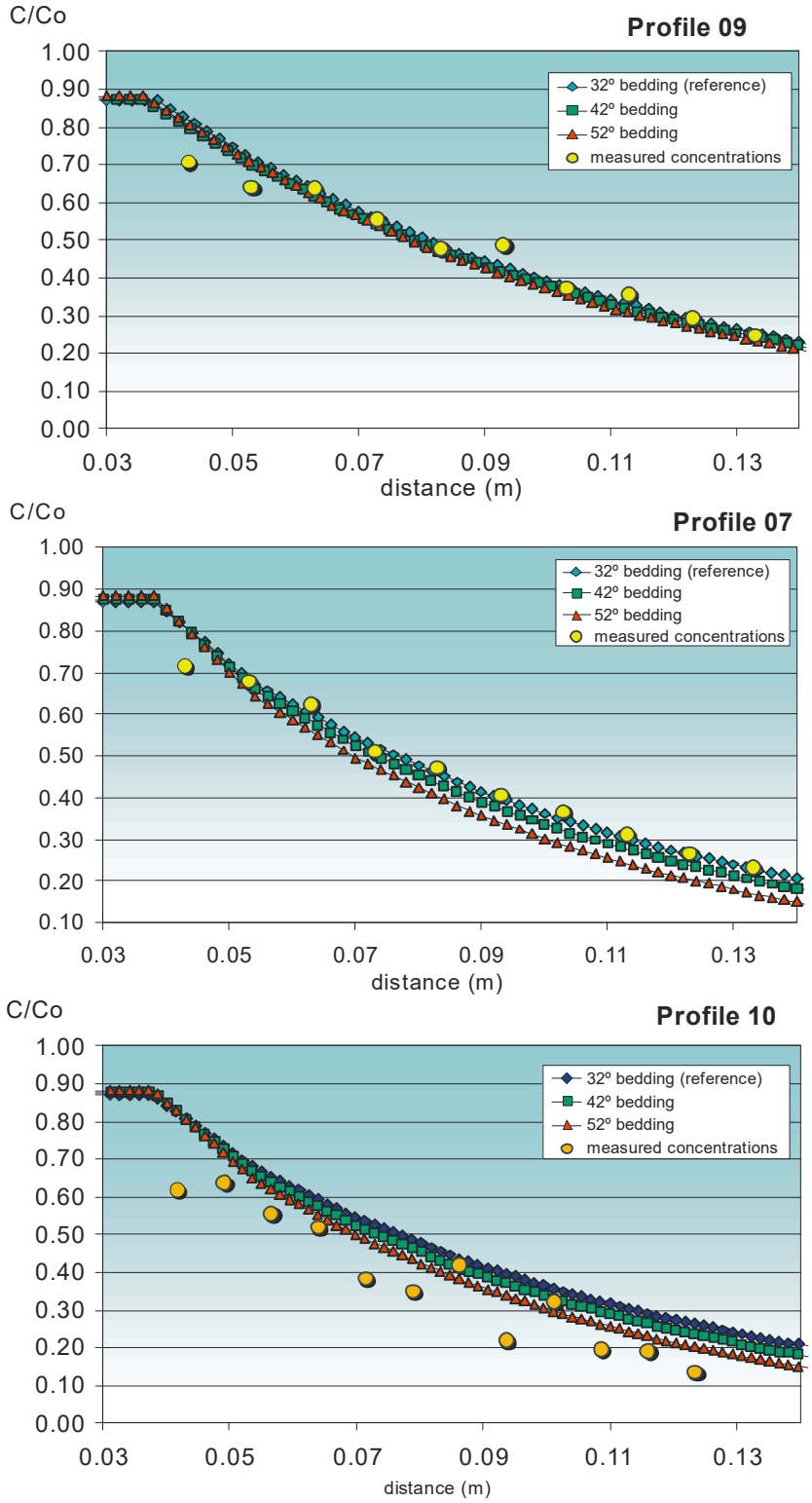

Fig. 10. Sensitivity analysis of HDO computed concentrations to variation of bedding angle. Relative concentrations are presented against horizontally projected distance to borehole axis.

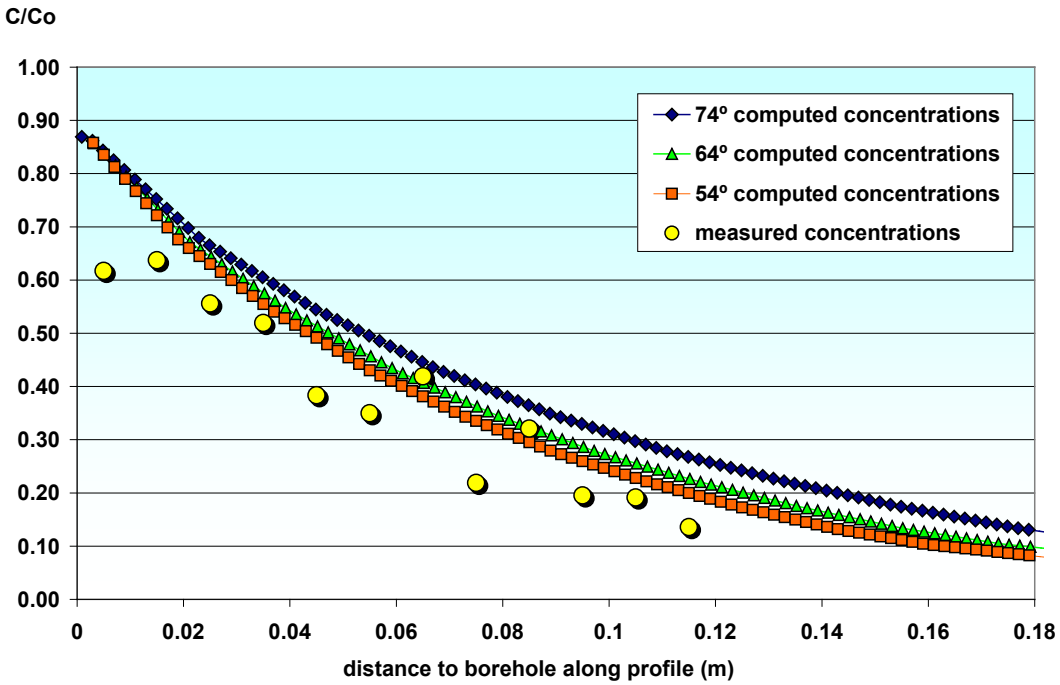

Fig. 11. Fit of HDO computed concentrations to measured data for profile 10, considering different values of the angle between profile direction and bedding plane.

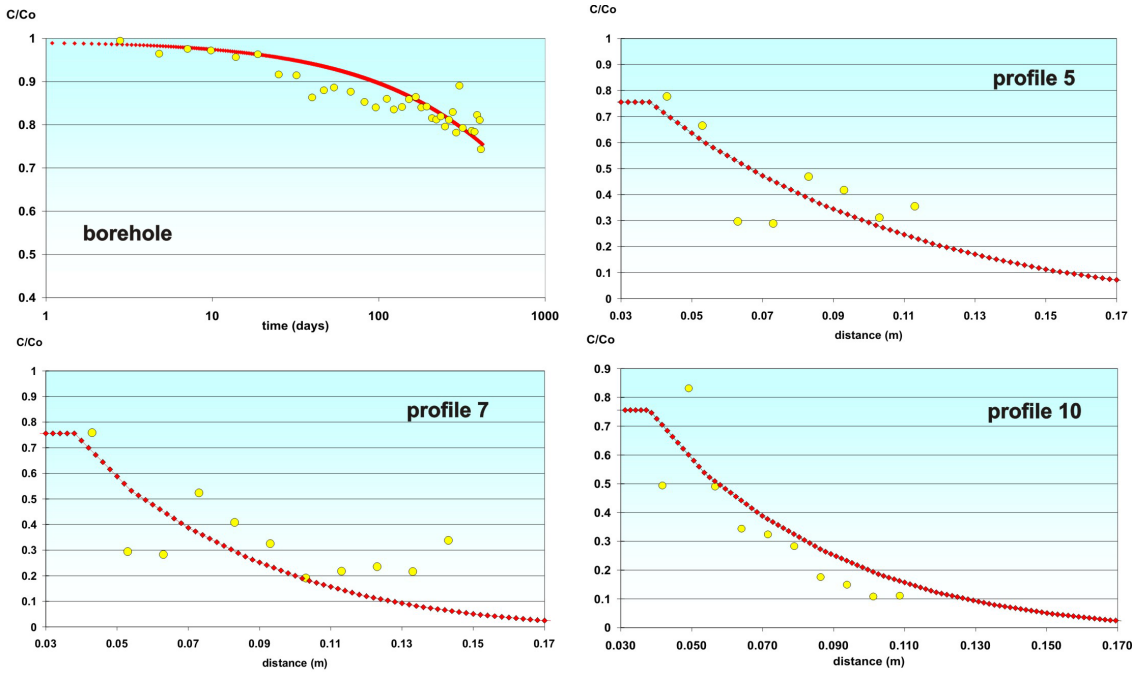

Fig. 12. Fit of $^{6}Li^{+}$ computed concentrations to measured data into the borehole and along profiles in different directions at the end of the experiment. All concentrations are relative concentrations in solution (C/C_0). Distance is with respect to borehole axis (borehole radius = 0.038 m).

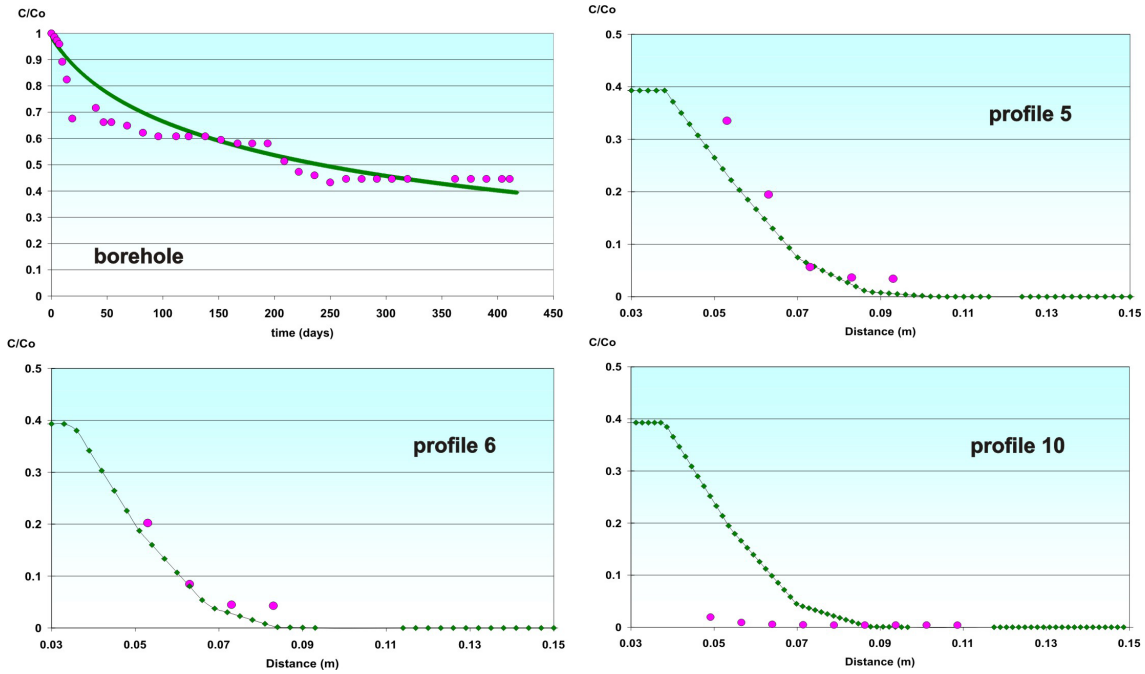

Fig. 13. Fit of $^{87}Rb^{+}$ computed concentrations to measured data into the borehole and along profiles of different directions at the end of the experiment. All concentrations are relative concentrations in solution (C/C_0). Distance is with respect to borehole axis (borehole radius = 0.038 m).

Acknowledgements

Financial support from Enresa and Nagra is gratefully acknowledged.

References

Bear J. (1972) Dynamics of Fluids in Porous Media. Elsevier.

Degueldre, C., Scholtis, A., Laube, A., Turrero, M.J., Thomas, B., 2003. Study of pore water chemistry through an argillaceous formation: a paleohydrochemical approach. Appl. Geochem.18 (1), 55 - 73.

Moriguti, T., Nakamura, E. (1998) High-yield lithium separation and the precise isotopic analysis for natural rock and aqueous samples. Chem. Geol. 145, 91-104.

Palut, J.-M., Montarnal, P., Gautschi, A., Tevissen, E., Mouche, E., 2003. Characterisation of HTO diffusion properties by an in-situ tracer experiment in Opalinus Clay at Mont Terri. J. Contam. Hydrol. 61, 203 - 218.

Pearson, F. J., Arcos, D., Bath, A., Boisson, J.-Y., Fernández, A. M., Gäbler, H.-E., Gaucher, E., Gautschi A., Griffault L., Hernán P., Waber H. N. (2003) Mont Terri Project – Geochemistry of Water in the Opalinus Clay Formation at the Mont Terri Rock Laboratory. Reports of the FOWG (Federal Office of Water and Geology), Geology Series, No. 5. Bern, Switzerland.

Rübel, A.P., Sonntag, C., Lippmann, J., Pearson, F.J., Gautschi, A., 2002. Solute transport in formations of very low permeability: profiles of stable isotope and dissolved gas contents of pore water in the Opalinus Clay, Mont Terri, Switzerland. Geochim. Cosmochim. Acta 66, 1311 - 1321.

Samper, J., Yang, C., Naves, A., Molinero, J., 2007. Modelización del Ensayo de Difusión In Situ DI-B Realizado en la Formación Opalinus Clay en el Laboratorio de Mont Terri (Suiza). Universidade da Coruña, Final Report.

Samper, J., Yang, C., Naves, A., Yllera, A., Hernández, A., Molinero, J., Soler, J.M., Hernán, P., Mayor, J.C., Astudillo, J. (2006) A fully 3-D anisotropic numerical model of the DI-B in situ diffusion experiment in the Opalinus Clay formation. Physics and Chemistry of the Earth 31, 531-540.

Sanz, H., Wasserburg, G.J. (1969) Detremination of an internal 87Rb/87Sr isochrone for the Olivenza chondrite. Earth Planet. Sci. Letters 6, 335-345.

Steefel, C.I. (2006) CrunchFlow, Software for Modeling Multicomponent Reactive Flow and Transport. User's Manual. Lawrence Berkeley National Laboratory, USA.

Steefel, C.I. (2001) GIMRT, Version 1.2: Software for Modeling Multicomponent, Multidimensional Reactive Transport. User's Guide, UCRL-MA-143182. Livermore, California: Lawrence Livermore National Laboratory.

Steefel, C.I., Yabusaki, S.B. (1996) OS3D/GIMRT, Software for Multicomponent-Multidimensional Reactive Transport: User's Manual and Programmer's Guide, PNL-11166, Pacific Northwest National Laboratory, Richland, Washington.

Tevissen E., Soler J. M., Montarnal P., Gautschi A., Van loon L. (2004) Comparison between in situ and laboratory diffusion dtudies of HTO and halides in Opalinus Clay from the Mont Terri. Radiochimica Acta 92, 781-786.

Van Loon, L.R., Soler, J.M., Müller, W., Bradbury, M.H. (2004a) Anisotropic diffusion in layered argillaceous formations: a case study with Opalinus clay. Environmental Science and Technology, 38, 5721-5728.

Van Loon, L.R., Wersin, P., Soler, J.M., Eikenberg, J., Gimmi, Th., Hernán, P., Dewonck, S., Savoye S. (2004b) In-situ diffusion of HTO, $^{22}Na^{+}$, Cs^{+} and I^{-} in Opalinus Clay at the Mont Terri underground rock laboratory. Radiochimica Acta 92, 757-763.

Wersin, P., Baeyens, B., Bossart, P., Cartalade, A., Dewonck, S., Eikenberg, J., Fierz,T., Fisch, H.R., Gimmi, T., Grolimund, D., Hernán, P., Möri, A., Savoye, S., Soler, J., van Dorp, F., Van Loon, L. (2006) Long-Term Diffusion Experiment (DI-A): Diffusion of HTO, I-, 22Na+ and Cs+. Field Activities, Data and Modelling. Mont Terri Technical Report 2003-06.

Wersin P., Soler J. M., Van Loon L., Eikenberg J., Baeyens B., Grolimund D., Gimmi T., Dewonck (2007) Diffusion of HTO, I^{-}, Cs^{+}, $^{85}Sr^{2+}$ and $^{60}Co^{2+}$ in a clay formation: Results and modelling from an in-situ experiment in Opalinus Clay. Applied Geochemistry (submitted).

Wersin P., Van Loon L. R., Soler J. M., Yllera A., Eikenberg J., Gimmi Th., Hernán P., Boisson J. Y. (2004) Long-term diffusion experiment at Mont Terri: First results from field and laboratory data. Applied Clay Science 26, 123-135.

Yang, C., Juanes, R., Samper, J., Molinero, Montenegro, L. (2003) User's Manual of $CORE^{3D}$. Technical Report, University of La Coruña, Spain.

Yllera, A., Hernández, A., Mingarro, M., Quejido, A., Sedano, L.A., Soler, J.M., Samper, J., Molinero, J., Barcala, J.M., Martín, P.L., Fernández, M.,Wersin, P., Rivas, P., Hernán, P. (2004) DI-B experiment: planning, design and performance of an in situ diffusion experiment in the Opalinus Clay formation. Applied Clay Science 26, 181–196.

You, C.-F., Chan, L.-H. (1996) Precise determination of lithium isotopic composition in low concentration natural samples. Geochim. Cosmochim. Acta 60, 909-915.